

## Proteomic evaluation of the response of soybean (*Glycine max* var *Seoritae*) leaves to UV-B Sung-Eun Lee<sup>1,\*</sup>, Sung Yung Yoo<sup>2,\*</sup>, Do-Yeon Kim<sup>2</sup>, Tae Seok Ko<sup>2</sup>, Yong Sik Ok<sup>3</sup>, Tae-Wan Kim<sup>2,\*\*</sup>

<sup>1</sup>School of Applied Biosciences, Kyungpook National University, Daegu 702-701, Korea

<sup>2</sup>Institute of Ecological Phytochemistry, Department of Plant Life & Environmental Science, Hankyong National University, Anseong 456-749, Korea

<sup>3</sup>Department of Biological Environment, Kangwon National University, Chuncheon 200-701, Korea

\*Authors contributed equally to this paper.

\*\*Corresponding author: taewkim@hknu.ac.kr

### Abstract

UV-B radiation plays an important role in photomorphogenesis; however, excessive UV-B radiation decreases photosynthesis and causes damage to cellular DNA. In the present study, two different light sources (UV-B and natural light) were applied to 18 day-old young soybean plants (*Glycine max* Merr. var *Seoritae*), after which the plants were harvested and their pigment contents, chlorophyll fluorescence, and proteomic changes investigated. The contents of carotenoids and anthocyanins increased significantly in response to excessive UV-B radiation. Additionally, several proteins such as ATP synthase, sedoheptulose-1,7-bisphosphatase, transketolase, peroxiredoxins and oxygen-evolving enhancer proteins were up-regulated in soybean leaves exposed to excessive UV-B. Alanine-2-oxoglutarate aminotransferase 1, aldolase, gamma-glutamyl hydrolase, and 28 kDa stem glycoprotein were down-regulated in soybean leaves exposed to excessive UV-B. Excessive UV-B light also led to a dramatic reduction in photosynthetic efficiency when compared to controls by causing irreversible damage to PSII determined by a fluorescence imaging system. With the treatment of natural illumination, the contents of carotenoids and anthocyanins were not changed in the leaves and the photosynthetic ability in the natural light was retained. These findings indicate that *Seoritae* soybean leaves might protect themselves from excessive UV-B radiation via up-regulation of antioxidative proteins and antioxidant pigments.

**Keywords:** UV-B; *Glycine max* Merr. var *Seoritae*; proteomics; pigments; fluorescence images; photosynthetic efficiency

### Introduction

Severe climate changes in Korea have led to an increase in average temperature of 1.5°C over the last 100 years, which has resulted shorter winters and longer summers (Kim et al., 2010). Other climate changes in Korea include a decrease in ozone by as much as -3.8% per decade (Kim et al., 2005), which can lead to increased ultraviolet (UV)-B radiation (Kerr et al., 1993). Additionally, climate change is known to reduce the production of agricultural commodities and infrastructure (Kim et al., 2012). UV-B radiation (280-320 nm) is one of the most destructive environmental factors for plants. Photosynthesis process converts light energy to chemical energy, and chlorophylls act as the primary absorbers of energy within a plant. Enhancement of UV-B radiation by ozone depletion may cause severe damage to photosynthetic systems (PS) via PSII dysfunction (Krause et al., 1999), which may occur as a result of changes in expression of photosynthesis-related proteins and defensive proteins in damaged plant leaves. Proteomics using two-dimensional polyacrylamide gel-electrophoresis (2D-PAGE) for protein separation in conjunction with mass spectroscopy analysis for peptides can be used to compare protein expression in target samples to those of controls. Proteomic analysis has been employed in investigations of the effects of UV-B radiation on photosynthesis to determine the differential expression of proteins in maize (Casati et al., 2011), soybeans (Xu et al., 2008) and radish (Singh et al., 2010), as well as some photosynthetic bacteria including *Synechocystis*

sp. PCC 6803 (Gao et al., 2009) and *Anabaena doliolum* (Mishra et al., 2009). Investigation of the up-regulation of defense mechanisms in plants protecting themselves from UV-B radiation has revealed antioxidant proteins such as peroxidase, superoxide dismutase, catalase, and glutathione reductase (Singh et al., 2010), as well as secondary metabolites such as glucosinolates, flavonol glycosides and carotenoids (Middleton and Teramura, 1993; Singh et al., 2010; Mewis et al., 2012). Inhibition of thermal energy dissipation is another effect of UV-B on photosynthesis (Moon et al., 2011); thus, identification of changes in thermal energy dissipation in plant leaves can help understand UV-B effects. For example, non-photochemical quenching (NPQ) of chlorophyll fluorescence indicates thermal dissipation of excitation energy absorbed for photosynthesis (Moon et al., 2011). Therefore, determination of changes in NPQ and other chlorophyll fluorescence parameters may be a good tool for determination of UV-B radiation effects on photosynthesis in damaged plant leaves. In the present study, we examined the effects of UV-B radiation on photosynthesis in soybean seedlings that were exposed to UV-B radiation for 3 days. Since UV-B radiation affects photosynthesis, we analyzed dysfunction of photosynthetic systems using chlorophyll fluorescence techniques. To accomplish this, the leaves of damaged soybean seedlings were collected and subjected to proteomic analysis using 2D-PAGE in conjunction with MALDI-TOF MS analysis. Changes in the proteome in

response to UV-B radiation resulted in dysfunction of photosynthesis in soybean seedlings. Additionally, increased levels of antioxidants were observed in response to UV-B in exposed soybean seedlings.

## Results and Discussion

Results of analysis of the pigment contents are given in Figs 1 and 2. Pigment contents were compared in plants subjected to UV-B (280-320nm) and natural light (moderate light) after being subjected to dark conditions for 3 days. Fig.1 shows changes in chlorophyll (chl) *a* and *b* contents and the chlorophyll *a/b* ratio under different light conditions. The content of chl *a* decreased rapidly during dark treatment, especially within the first 72 h. As shown in Fig. 1A, when soybean leaves were exposed to moderate light (natural light), the content of chl *a* increased significantly relative to the UV-B exposed leaves. However, the content of chl *a* under the UV-B radiation was reduced in comparison to the leaves under the dark condition. Chl *b* is known to be more sensitive to UV-B radiation than chl *a* (Strid and Porra, 1992). Signaling to senescence clearly progressed in plants subjected to dark and UV-B treatments, indicating chlorophyll degradation (Fig. 1B). In general, reductions in chlorophyll are indicative of stress and senescence (Richardson, 2002; Young et al., 1990). Chl *a/b* has frequently been used as an indicator of plant response to light intensity (Hendry and Price, 1993). In the present study, the Chl *a/b* ratio (Fig. 1C) decreased gradually under dark conditions, and the ratio was significantly lower in UV-B exposed leaves than in those exposed to natural light (Fig 1C). Carotenoids and anthocyanins were dramatically upregulated in soybean leaves exposed to UV-B radiation. Specifically, the levels of these two pigments were significantly higher in UV-B exposed soybean leaves than in those exposed to natural light (Fig. 2). Carotenoids were not determined under dark conditions (Fig. 2A). Similarly, anthocyanin content was significantly enhanced in soybean leaves after exposure to UV-B radiation (Fig. 2B). Taken together, these findings show that the induction of carotenoid and anthocyanin biosynthesis was triggered by exposure of UV-B radiation rather than natural light illumination, indicating that these compounds are related to the removal of oxidative stresses initiated by UV-B radiation (Fig. 2). Close et al. (2003) recently showed that anthocyanins protected against photo-damage. In addition to the photoprotection afforded by anthocyanins, carotenoids are also known to play a significant role in photoprotection of photosynthetic membranes against large amounts of solar energy absorbed by photosynthetic pigments (González et al., 2007). Therefore, these two pigments are generated to protect against photo-damage in soybean leaves subjected to UV-B radiation. The minimal level of fluorescence ( $F_0$ ) is the fluorescence in the absence of photosynthetic light. A significant increase in  $F_0$  indicates impairment of regulatory processes in the reaction center of PSII as a result of light stress. Maximal fluorescence ( $F_m$ ) is the level of fluorescence when PSII is fully closed. No significant differences in  $F_0$  values were observed under dark conditions. However, plants subjected to different light sources showed a significant difference in  $F_0$  values at 48 h after irradiation (Fig. 3A), with  $F_m$  values being significantly higher in response to natural light than to UV-B radiation (Fig. 3B). The lower levels in the UV-B exposed leaves indicated damage to the reaction center and antenna of PSII (Fig. 3A and B). The quantum efficiencies or yield ( $F_v/F_m$ ) values were higher in leaves subjected to natural light than in those subjected to UV-B radiation (Fig. 3C). Henley et al. (1991) demonstrated an increase in  $F_0$  and a decrease in  $F_m$  after exposure to high fluorescence rates of solar light. Additionally, Havaux (1993) showed that increased

$F_0$  values could be interpreted as a reduction in the rate constant of energy trapping by PSII centers, which could be a result of physical dissociation of the light harvesting complex from the PSII core as has been observed in plants damaged by stress (Armond et al., 1980). Decreased  $F_m$  values reflect a reduction in the ability of PSII to reduce the primary acceptor QA (Calatayud and Barreno, 2001).  $F_m$  values are also known to decrease due to abiotic stresses (Panda et al., 2008); therefore, the changes in  $F_0$  and  $F_m$  values observed in soybean leaves in the present study indicate damage caused by light stress. The decrease in  $F_v/F_m$  was associated with changes in  $F_0$  and  $F_m$  as a result of increased  $F_0$  (Fig. 3A) and reduced  $F_m$  and  $F_v$  (Fig. 3B and C). Therefore, it is likely that the decrease of  $F_v/F_m$  (Fig. 4A) was related to the loss of chlorophyll associated with PSII and the light-harvesting complex of PSII in response to light stresses. The result of  $F_v/F_m$  correlated with UV-B radiation and moderate light condition except lightening for 4 h. Upon exposure to excess light, the D1 protein of the PSII reaction center was inactivated by phosphorylation and then degraded, leading to an inactive PSII center.  $F_v/F_m$  can be used as an indicator of this process since there is a good correlation between degradation of D1 protein measured by radioactive labeling and  $F_v/F_m$  (Rintamaki et al., 1995). In healthy leaves, the  $F_v/F_m$  value is always close to 0.8, while a lower value indicates that a proportion of PSII reaction centers are damaged. Such damage is known as photo-inhibition, and often observed in plants under these conditions. The PSII operating efficiency ( $\Phi_{PSII}$ ) was reduced rapidly under dark conditions (Fig. 5), while it increased following exposure to normal light, indicating a recovery from light stress. However, this did not occur when UV-B radiation was applied to soybean seedlings following exposure to dark conditions (Fig. 5), indicating that UV-B radiation prevented recovery of PSII from light stress (Fig. 5). The greatest difference between moderate light-treated and UV-B treated soybean seedlings was observed after 24 and 72 h of exposure to the light treatments. Non-photochemical quenching (NPQ) of chlorophyll fluorescence indicates dissipation of excess excitation energy as heat during photosynthesis. Therefore, the occurrence of NPQ helps control abnormal photosynthesis as a result of excessive absorption of light energy. In the present study, NPQ was found to play an important role in restoration of PSII function following exposure to normal light (Fig. 6). Specifically, NPQ decreased significantly in response to UV-B light (Fig. 6), indicating that it helped dissipate excess energy from the photosystem and that the function of PSII was strongly inhibited by light stresses. Chlorophyll fluorescence images were analyzed to investigate the photosynthetic efficiency (Figs. 7 and 8). On the images, higher energy fluorescence appeared red and lower as blue.  $F_0$  emitted high energy and the  $F_v/F_m$  was maintained at a low level during 48 h of dark treatment (Fig. 7), clearly indicating that radiant energy quantity increased, whereas the utilization of photosynthesis decreased.  $\Phi_{PSII}$  was also reduced during 48h of dark exposure. However, these values were all recovered upon exposure to moderate light. Conversely, the photosynthetic ability was severely damaged by UV-B light after dark treatment for 72 h (Figs7 and 8); therefore, the soybean leaves lost their photosynthetic capacity. About 400 proteins spots were separated by 2-D PAGE and analyzed by the PD-QUEST program to compare protein expression among treatments. The 2-D PAGE gels were reproducible and five representative gels are presented in Fig. 9. Each gel contains all proteins expressed under dark treatment (0, 48, and 72 h), UV-B (72 h), and moderate light illumination (72 h). Only spots that were significantly affected by UV-B (Fig. 9D) or moderate light (Fig. 9E) when compared to spots (Fig. 9C) expressed at

**Table 1.** Identification of proteins differentially expressed in soybean leaves after exposure to UV-B for 3 days. The spot number indicates the same number as in Fig.10. D indicates decreased expression, whereas no prefix indicates increased expression.

Spot No	Protein	Mascot score (P=0.05)	Function
1	ATP synthase beta subunit	95 (48)	ATP hydrolysis coupled proton transport
2	Ribulose-1,5-bisphosphate carboxylase	86 (51)	Photorespiration
3	Trypsin	-	-
4	Trypsin	-	-
5	Sedoheptulose-1,7-bisphosphatase	88 (74)	Carbohydrate metabolic pathway
6	Trypsin	-	-
7	No match	-	-
8	Oxygen-evolving enhancer protein 2, chloroplast precursor (OEE2)	83 (51)	Photosynthesis, light reaction
9	ATP synthase CF1 epsilon subunit	272 (62)	ATP hydrolysis coupled proton transport
10	No match	-	-
11	No match	-	-
12	No match	-	-
13	Ribulose-1,5-bisphosphate carboxylase small subunit rbcS1	121 (52)	Photorespiration
14	Peroxioredoxin	126 (52)	Response to oxidative stress
15	Large subunit of ribulose-1,5-bisphosphate carboxylase/oxygenase	65 (52)	Photorespiration
16	No match	-	-
17	Oxygen-evolving enhancer protein 2	83 (51)	Photosynthesis, light reaction
18	Oxygen-evolving enhancer protein 2	83 (51)	Photosynthesis, light reaction
19	ATP synthase CF1 epsilon subunit	272 (62)	ATP hydrolysis coupled proton transport
20	Rubisco	56 (52)	Photorespiration
21	Ribulose-1,5-bisphosphate carboxylase/oxygenase large subunit	195 (52)	Photorespiration
22	Ribulose-1,5-bisphosphate carboxylase/oxygenase large subunit	135 (51)	Photorespiration
23	RuBisCO small subunit	69 (51)	Photorespiration
24	No match	-	-
25	Peroxioredoxin	134 (62)	Response to oxidative stress
26	Ribulose-1,5-bisphosphate carboxylase/oxygenase large subunit	69 (52)	Photorespiration
27	No match	-	-
28	Ribulose-1,5-bisphosphate carboxylase small subunit rbcS1	136 (51)	Photorespiration
D1	Transketolase	81 (52)	Growth
D2	Photosystem II oxygen-evolving enhancer protein 2	87 (52)	Photosynthesis, light reaction
D3	Rubisco large subunit-binding protein subunit alpha, CPN-60 alpha	326 (52)	Protein refolding
D4	Ribulose-1,5-bisphosphate carboxylase/oxygenase large subunit	61 (52)	Photorespiration
D5	ATP synthase CF1 beta subunit	1125 (48)	ATP hydrolysis coupled proton transport
D6	Alanine-2-oxoglutarate aminotransferase 1 (GGT 1)	93 (61)	Response to hypoxia, L-alanine catabolic pathway
D7	Gamma-glutamyl hydrolase precursor	96 (52)	Glutamine metabolic process
D8	Homologous to plastidic aldolases or chloroplast latex aldolase-like protein	126 (51)	Cofactor metabolic process
D9	LH II type I chlorophyll a/b binding protein	236 (52)	Photosynthesis, light harvesting
D10	Gamma-glutamyl hydrolase precursor (Gamma-Glu-X carboxypeptidase)	264 (51)	Glutamine metabolic process
D11	Stem 28 kDa glycoprotein precursor	153 (51)	Acid phosphatase activity
D12	23 kDa subunit of oxygen evolving system of photosystem II	72 (51)	Photosynthesis, light reaction
D12	Oxygen evolving enhancing protein II	93 (52)	Photosynthesis, light reaction
D13	Chloroplast small heat shock protein	168 (52)	Response to stress
D14	18.0 kDa class I heat shock protein	93 (51)	Response to stress
D15	No match	-	-
D16	Ribulose 1,5-bisphosphate carboxylase [ <i>Zingiber gramineum</i> ]	269 (52)	Photorespiration
D17	Ribulosebisphosphate carboxylase large chain precursor	61 (51)	Photorespiration
D18	No match	-	-

72 h duration after dark treatment were further analyzed. A total of 46 spots differently expressed under UV-B illumination were selected by image analysis (PD-QUEST) (Fig. 10). A total of 25 spots differently expressed under moderate light illumination were selected by image analysis (Fig. 11). The proteins up- and down-regulated in response to different light conditions are listed in Tables 1 and 2 with numberings that are presented in Fig. 10 for UV-B illumination and Fig. 11 for moderate light illumination. Ribulosebiphosphate carboxylase/oxygenase (Rubisco) and oxygen evolving enhancer protein (OEE) were predominantly found in this study, which is typical of such investigations. Illumination with UV-B for 72 h increased ATP synthase beta subunit, Rubisco, OEE2, and peroxiredoxin expression, but decreased transketolase, Rubisco, ATP synthase, alanine-2-oxoglutarate aminotransferase, gamma-glutamyl hydrolase, plastidaldolases, 28kDa glycoprotein precursor, OEE, chloroplast small heat shock protein, class I heat shock protein, and chlorophyll a,b-binding protein (Table 1). Illumination with moderate light for 72 h increased heat shock protein 70, glutamine synthetase precursor, fructose-biphosphatealdolase 2, glycerate 3-phosphate dehydrogenase, Rubisco, stem 31 kDa glycoprotein precursor, and chlorophyll a,b-binding protein, but decreased expression of peroxiredoxin and chloroplast heat shock protein (Table 2). Chlorophyll a,b-binding protein decreased under UV-B illumination, but increased under moderate light illumination. Peroxiredoxin expression was up-regulated under UV-B illumination, but down-regulated under moderate light illumination. Xu et al. (2008) found that 67 proteins in soybean leaves were significantly affected by solar UV-B. Among the differently expressed proteins, 31 increased, including gamma-glutamyl hydrolase, Rubisco, triosephosphateisomerase, OEE proteins, 50S ribosomal protein, 30S ribosomal protein, vegetative storage proteins, ascorbate peroxidase, superoxide dismutase, and some unidentified proteins. Conversely, 36 proteins decreased, including alanine aminotransferase, glutamate synthetase, Rubisco, GAPDHs, carbonic anhydrases, chaperonins, catalase, peroxiredoxin, and chalconeredutase. These results are very similar to our results, except for the expression of several proteins including gamma-glutamyl hydrolase, ATP synthase, peroxiredoxins, transketolase, and glycoproteins (Tables 1 and 2). Our findings regarding the expression of gamma-glutamyl hydrolase and peroxiredoxins were different from those reported by Xu et al. (2008) in that our unpublished results demonstrated that down-regulation of the expression of gamma-glutamyl hydrolase and peroxiredoxins was related to light illumination. As shown in Fig. 9B and C, gamma-glutamyl hydrolase and peroxiredoxins decreased significantly in the absence of light exposure. Further studies are required to elucidate the reasons for this discrepancy among studies. The down-regulation of transketolase and alanine-2-oxoglutarate aminotransferase expression under UV-B exposure is also interesting. Transketolase is a key enzyme involved in mediation of the reversible transfer of a glycoaldehyde group from a donor ketose (xylulose-5-phosphate) to an acceptor aldose (ribose-5-phosphate or erythrose-4-phosphate), resulting in the formation of glyceraldehyde 3-phosphate and sedoheptulose-7-phosphate (Schenk et al., 1998). Therefore, the down-regulation of transketolase by UV-B exposure caused reduced production of glyceraldehyde 3-phosphate, which likely affected the glycolytic pathways. Conversely, glycerate-3-phosphate dehydrogenase in soybean leaves was up-regulated under moderate light exposure. These findings indicate that normal light conditions may enhance the glycolysis pathway in soybean leaves when compared to both dark and UV-B conditions, enabling production of glucose and energy from

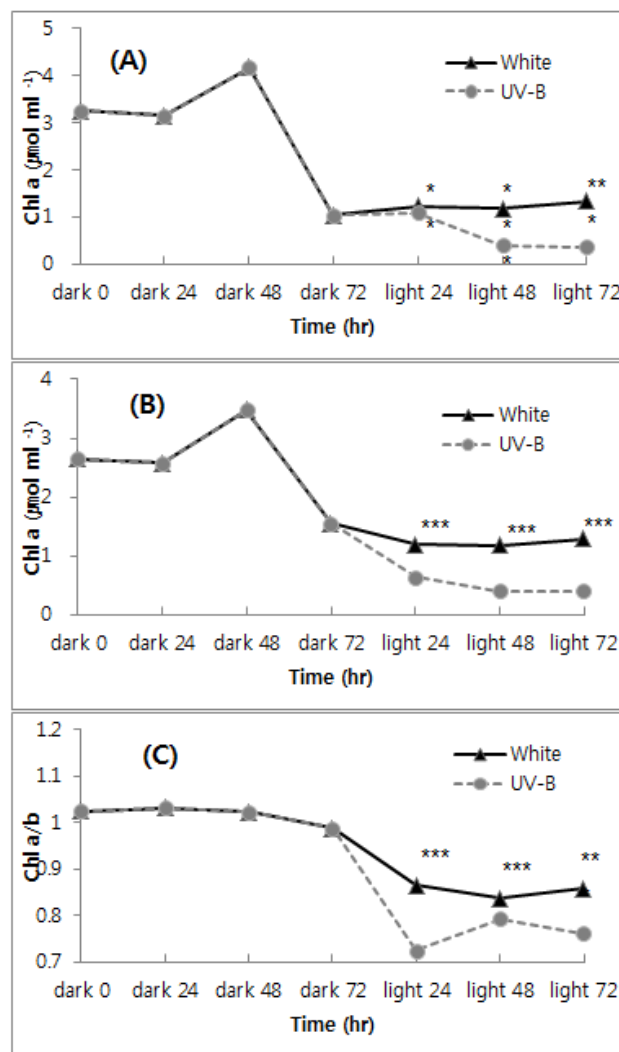


**Fig 1.** Effects of treatment with moderate light and UV-B for 3 days after 3 days of growth under dark conditions on chlorophyll *a* content (A), chlorophyll *b* content (B) and chlorophyll *a/b* ratio (C) in soybean. All units are in  $\mu\text{mol ml}^{-1}$ . \*\*\*, \*\* and \* represent significant differences at  $p < 0.001$ ,  $p < 0.01$  and  $p < 0.05$ , respectively, as determined by a Student's *t*-test. Diamonds and solid lines indicate moderate light and rectangles and dotted line indicate UV-B light.

sunlight (Table 1). Fructose-biphosphatealdolase was also found to be upregulated under moderate light exposure. Overall, these findings indicate that the two different light sources may cause different levels of final products of photosynthesis such as glucose and energy. Recently, a peroxiredoxin gene from *Panax ginseng* leaves was isolated under UV-B oxidative stress (Kim et al., 2010). Similarly, a peroxiredoxin, Prdx6, was found to play an important role in UV-B radiation exposure in *Prdx6<sup>+/+</sup>* and *Prdx6<sup>-/-</sup>* mouse (Kubo et al., 2010). These reports suggest that peroxiredoxins are essential to protection of host organisms from oxidative stresses caused by UV-B radiation, which can lead to overproduction of reactive oxygen species (ROS). In the present study, UV-B exposed soybean leaves up-regulated the expression of peroxiredoxin, which may play an important role in the protection of host cells from ROS. Finally, the expression of LH II type I chlorophyll a,b-binding protein was controlled by exposure to different light source (Tables 1 and 2). This protein is known to be exclusively associated with photosystem II as a light harvester (Jansson,

**Table 2.** Identification of proteins differentially expressed in soybean leaves after exposure to natural light for 3 days. The spot number indicates the same number as in Fig.11. D indicates decreased expression, whereas no prefix indicates increased expression.

Spot No.	Protein	Mascot score (P=0.05)	Function
1	Heat shock protein 70	275 (52)	Response to stress
2	Rubisco	93 (61)	Photorespiration
3	Glutamine synthetase precursor	81 (51)	Glutamine biosynthetic process
4	No match	-	-
5	Fructose-bisphosphate aldolase 2, chloroplast	110 (52)	Glycolysis
6	Glycerate 3-phosphate dehydrogenase, chloroplast	91 (52)	Glycolysis
7	No match	-	-
8	Rubisco	56 (52)	Photorespiration
9	Ribulose-1,5-bisphosphate carboxylase/oxygenase large subunit	88 (52)	Photorespiration
10	Stem 31 kDa glycoprotein precursor	128 (51)	Acid phosphatase activity
11	Chlorophyll a,b-binding protein	126 (70)	Photosynthesis, light harvesting
12	No match	-	-
13	Rubisco large subunit	289 (51)	Photorespiration
14	Ribulose-1,5-bisphosphate carboxylase oxygenase	107 (52)	Photorespiration
15	Ribulose-1,5-bisphosphate carboxylase oxygenase [ <i>Sarcococca confusa</i> ]	136 (51)	Photorespiration
16	Ribulosebisphosphate carboxylase small chain 1, chloroplast precursor (RuBisCO small subunit 1)	169 (51)	Photorespiration
17	Rubisco	124 (52)	Photorespiration
18	Ribulose 1,5-bisphosphate carboxylase [ <i>Zingiber gramineum</i> ]	269 (52)	Photorespiration
19	No match	-	-
D1	Alanine-2-oxoglutarate aminotransferase 1 (GGT 1)	93 (61)	Response to hypoxia, L-alanine catabolic pathway
D2	Ribulose-1,5-bisphosphate carboxylase/oxygenase large subunit	61 (52)	Photorespiration
D3	Chloroplast small heat shock protein	73 (52)	Response to stress
D4	Ribulosebisphosphate carboxylase large chain precursor	61 (51)	Photorespiration
D5	Ribulosebisphosphate carboxylase large chain precursor	278 (54)	Photorespiration
D6	Ribulose-1,5-bisphosphate carboxylase/oxygenase large subunit	61 (52)	Photorespiration

1994). In the present study, UV-B radiation down-regulated LH II type I chlorophyll a,b-binding protein, while moderate light up-regulated the protein. Therefore, UV-B radiation does not accept normal light-harvesting process, which might explain the lower efficiency of energy transfer when compared to moderate light conditions. In addition to the low efficiency of energy transfer, potential photo-damage to the photosynthetic systems via over-excitation may result in hyper-production of carotenoids for photo-protection (Britton, 1993), which would explain the increased production of carotenoids in UV-B exposed soybean leaves in the present study.

## Materials and Methods

### Plant materials and culture condition

Soybean cultivation was carried out in a greenhouse and a chamber at Hankyong National University (Ansung, Korea) using seeds of *Glycine max Merr.* var *Seoritae* collected from Korea. Seeds were grown in 400 ml rubber pots for 18 days on vermiculite and tap water at 30°C, after which they were grown in a dark chamber for three days. The plants were then subjected to either moderate light or ultraviolet-B for three days. Plants were harvested when the first trifoliates were observed for proteomics analysis and for measurement of antioxidant secondary metabolites (including pigment contents) and fluorescence kinetic quenching.

### Pigment content analysis

Chlorophylls and carotenoids were extracted using 80% acetone (v/v). Anthocyanin was extracted in 1% HCl in MeOH (v/v). The clear supernatant obtained after filtration through two layers of cheesecloth was then centrifuged at 480 ×g for 3min (Lichtenthaler et al., 2007). Next, the samples were analyzed for absorbance at 663nm (chlorophyll a), 647nm (chlorophyll b), 470nm (carotenoids), and 537nm (anthocyanin) using a spectrophotometer (Beckman Coulter DU 650, CA) as described by Sims and Gamon (1999). All units are reported in  $\mu\text{mol ml}^{-1}$ .

### Measurement of fluorescence parameters

The fluorescence parameters were measured using a kinetic image fluorometer (Fluorcam 700MF) (Photon Systems Instruments, Brno, CZ) according to a protocol for quenching analysis. Briefly, the leaves were subjected to darkness for 30 min before measurement, after which they were exposed to continuous actinic light (red LED) at  $200 \mu\text{molm}^{-2}\text{s}^{-1}$  or saturating light (moderate light) at  $1250 \mu\text{molm}^{-2}\text{s}^{-1}$ . The majority of fluorescence measurements were made using a modulated fluorometer with the leaf poised in a known state. The procedures for making such measurements are shown in Fig.1, together with the fluorescence levels for a leaf in each specific state (Baker and Rosenqvist, 2004). Fluorescence parameters ( $F_0$ ,  $F_m$ ,  $F_v/F_m$  and  $\Phi\text{PSII}$ ) and the quenching

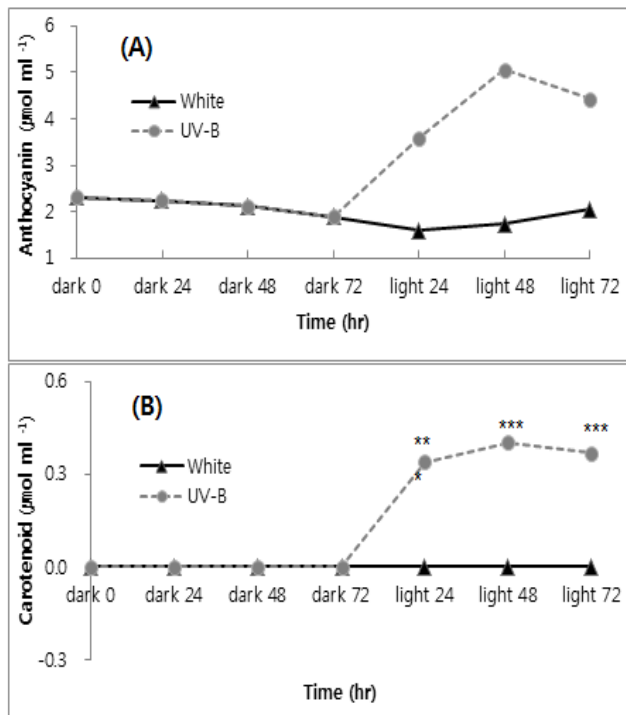


**Fig 2.** Effects of different light sources on carotenoid (A) and anthocyanin contents (B). All units are in  $\mu\text{mol ml}^{-1}$ . \*\*\* represent significant differences at  $p < 0.001$  as determined by a Student's *t*-test.

coefficients (NPQ) were then computed using the equations described by Schreiber et al. (1986).

### Proteomic analysis

#### Sample preparation and 2D-PAGE

Soybean seedling leaves at each step were prepared and 2D-PAGE was performed as described previously (Park et al., 2004). Briefly, soybean leaves were extracted with 0.5ml 50mM Tris buffer containing 7M urea, 2M thiourea, 4% (w/v) CHAPS, and 16 $\mu\text{l}$  protease inhibitor cocktail (Roche Molecular Biochemicals, Indianapolis, IN, USA). The lysates were then homogenized and centrifuged at 12,000  $\times$  g for 15 min. Next, 50 units of benzonase (250units/ $\mu\text{l}$  Sigma, St. Louis, MO, USA) were added to the mixture and it was stored at  $-80^{\circ}\text{C}$  until use after quantitation with Coomassie blue solution (BioRad, Hercules, CA, USA). For 2-DE analysis, pH 3-10 immobilized pH gradient (IPG) gel strips (Amersham Biosciences, Seoul, Korea) were rehydrated in swelling buffer containing 7M urea, 2M thiourea, 0.4% (w/v) DTT, and 4% (w/v) CHAPS. The protein lysates (500 $\mu\text{g}$ ) were then cup-loaded into the rehydrated IPG strips using a Multiphor II apparatus (Amersham Biosciences) for a total of 57kVh. Next, 2-D separation was performed on 8–16% (v/v) linear gradient sodium dodecyl sulfate-polyacrylamide gels. Following fixation of the gels for 1h in 40% (v/v) methanol containing 5% (v/v) phosphoric acid, the gels were stained with Colloidal Coomassie Blue G-250 solution (ProteomeTech, South Korea) for 5hr. The gels were then destained in 1% (v/v) acetic acid for 4hr, after which they were imaged using a GS-710 imaging calibrated densitometer (BioRad, Hercules, CA). Protein spot detection and 2-D pattern matching were carried out using the Image Master TM 2D Platinum software (Amersham Biosciences). For comparison of protein spot densities between

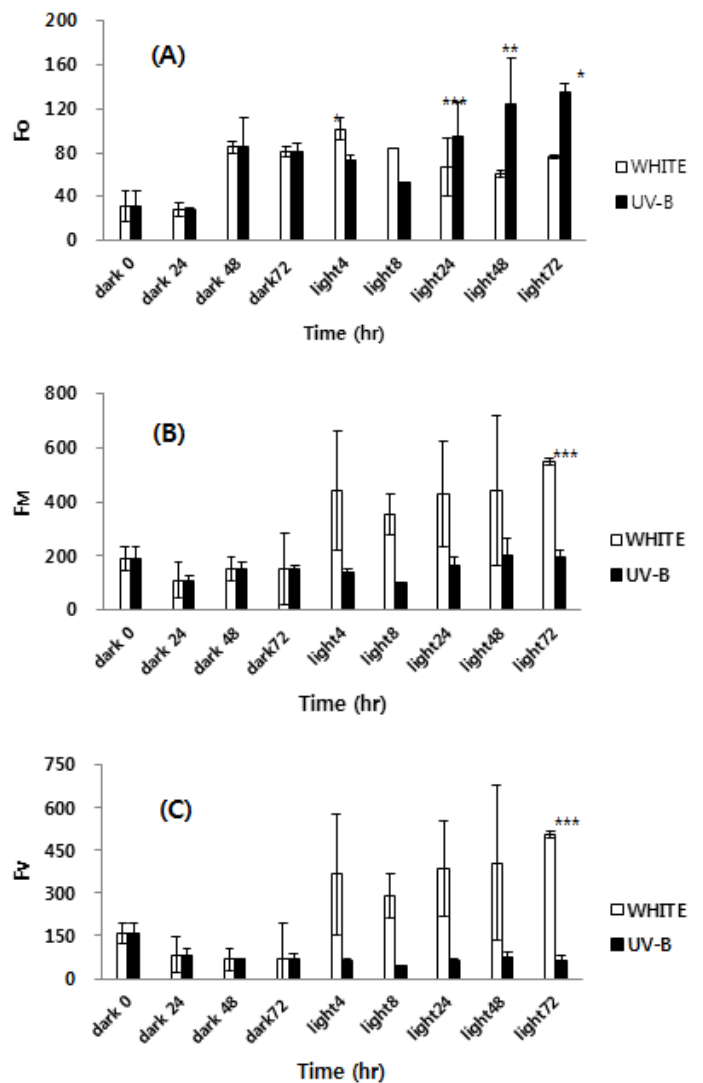


**Fig 3.** Changes in chlorophyll fluorescence parameters Fo (A), Fm (B) and Fv/Fm (C) in response to different light sources. \*\*\*, \*\* and \* represent significant differences at  $p < 0.001$ ,  $p < 0.01$  and  $p < 0.05$ , respectively, as determined by a Student's *t*-test.

control and treated samples, more than 20 spots throughout all gels were landmarked and normalized. The quantified spots of candidate proteins were compared with the aid of histograms. To ensure the reproducibility of 2-DE experiments, each sample was analyzed in duplicate.

#### In-gel digestion with trypsin and extraction of peptides

The procedure for in-gel digestion of protein spots was carried out as previously described (Park et al., 2004). Briefly, protein spots were excised from stained gels and cut into pieces that were subsequently washed for 1h at room temperature in 25mM ammonium bicarbonate buffer, pH 7.8, containing 50% (v/v) acetonitrile (ACN). Following dehydration of the gel pieces in a SpeedVac for 10 min, gel pieces were rehydrated in 10 $\mu\text{l}$  (20 ng/ $\mu\text{l}$ ) of sequencing grade trypsin solution (Promega, Madison, WI). After overnight incubation in 25mM ammonium bicarbonate buffer, pH 7.8, at  $37^{\circ}\text{C}$ , the tryptic peptides were extracted with 5  $\mu\text{l}$  of 0.5% TFA containing 50% (v/v) ACN for 40min with mild sonication. The extracted solution was then reduced to ca. 1 $\mu\text{l}$  in a vacuum centrifuge. Prior to mass

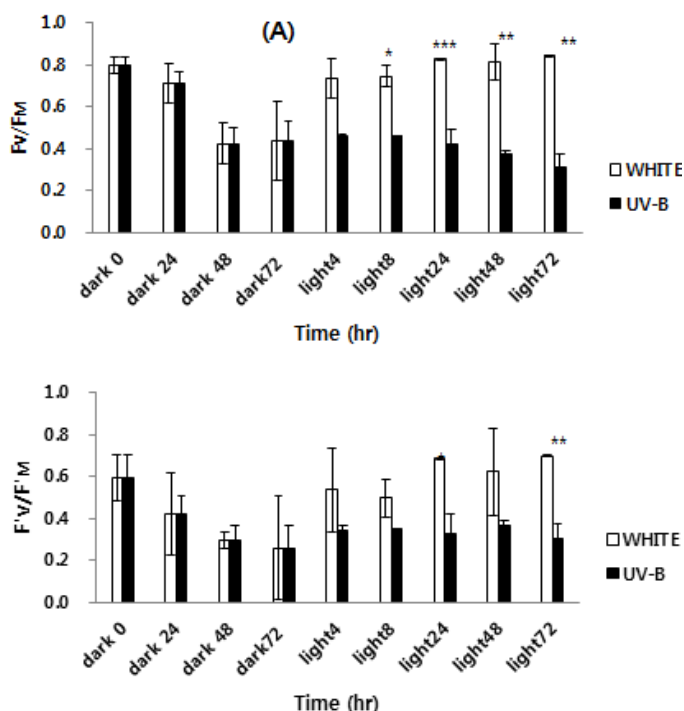


**Fig 4.** Changes in Fv/Fm (A) and F'v/F'm (B) yield in response to different light sources. \*\*\*, \*\* and \* represent significant differences at  $p < 0.001$ ,  $p < 0.01$  and  $p < 0.05$ , respectively, as determined by a Student's t-test.

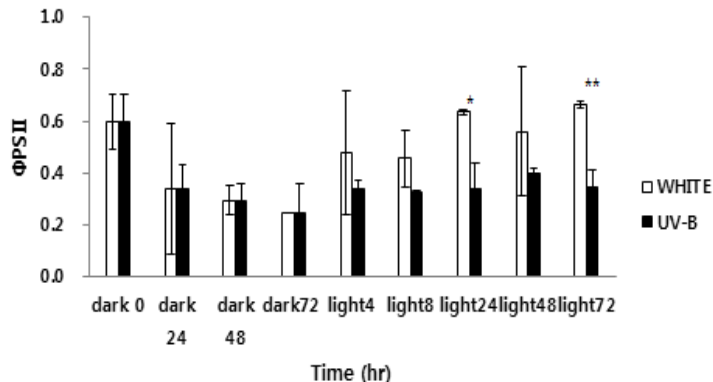


**Fig 5.** Changes in PSII operating efficiency ( $\Phi_{PSII}$ ) in response to different light sources. \*\* and \* represent significant differences at  $p < 0.01$  and  $p < 0.05$ , respectively, as determined by a Student's t-test.

spectrometric analysis, the resulting peptide solutions were subjected to a desalting process using a reversed-phase column (Gobom et al., 1999). To accomplish this, a constricted GEloder tip (Eppendorf, Hamburg, Germany) was packed with Poros 20 R2 resin (Perseptive Biosystems, Framingham, MA). After equilibration with 10  $\mu$ l of 5% (v/v) formic acid, the peptides solution was loaded onto the column and washed with 10  $\mu$ l of 5% (v/v) formic acid. The bound peptides were then eluted with 1  $\mu$ l of  $\alpha$ -cyano-4-hydroxycinnamic acid (CHCA) (5mg/mL in 50% (v/v) ACN/5% (v/v) formic acid) and dropped onto a MALDI plate (96  $\times$  2; Applied Biosystems, Forster City, CA).

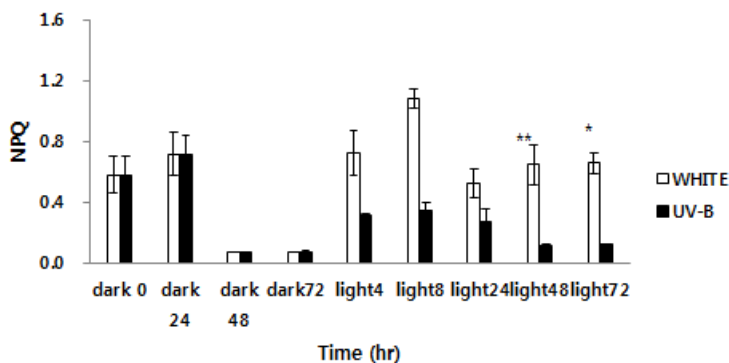


**Fig 6.** Changes in nonphotochemical quenching (NPQ) in response to different light sources. \*\* and \* represent significant differences at  $p < 0.01$  and  $p < 0.05$ , respectively, as determined by a Student's t-test.

#### Analysis of peptides by MALDI-TOF MS and identification of proteins

Mass measurement of tryptic peptides was carried out using a Voyager-DE STR mass spectrometer (Perspective Biosystems) in reflection positive ion mode as previously described (Bahk et al., 2004). Close external calibration was performed for every four samples using calibration mixtures of isotrophic fragment 18-39 (monoisotopic mass, 2465.1989), adrenocorticot neurotensin (mono-isotopic mass, 1672.9175), and angiotensin I (monoisotopic mass, 1296.6853) as standards, and mass spectra were acquired for the mass range of 900–3500 Da. The proteins were then identified by peptide mass fingerprinting searching against the Swiss-Prot and NCBI databases using the ProFound search program ([http://129.85.19.192/profound\\_bin/WebProFound.exe](http://129.85.19.192/profound_bin/WebProFound.exe), Rockefeller University, Version 4.10.5), MASCOT ([http://www.matrixscience.com/cgi/search\\_form.pl?FORMVER=2 & SEAR CH =PMF](http://www.matrixscience.com/cgi/search_form.pl?FORMVER=2 & SEAR CH =PMF)), or MS-Fit (<http://prospector.ucsf.edu/ucsfhtml4.0/msfit.htm>, University of California, San Francisco, Version 4.0.5). The following mass search parameters were set: peptide mass tolerance, 50ppm; a mass window between 0 and 100 kDa, allowance of missed cleavage, 2; consideration for variable modifications such as oxidation of methionine and propionamides of cysteines. Only significant hits defined by each program were considered initially, with at least four matching peptide masses.

#### Identification of proteins by LC-MS/MS

The resulting tryptic peptides were separated and analyzed using reversed phase capillary HPLC directly coupled to a Finnigan LCQ ion trap mass spectrometer (LC-MS/MS) (Zuo et al., 2001). A 0.1  $\times$  20 mm trapping and a 0.075  $\times$  130mm resolving column were both packed with Vydac 218MS low trifluoroacetic acid C18 beads (5  $\mu$ m diameter, 300 $\text{\AA}$  pore size; Vydac, Hesperia, CA) and placed in-line. The peptides were then bound to the trapping column for 10 min with 5% (v/v) aqueous acetonitrile containing 0.1% (v/v) formic acid, after which they were eluted with a 50 min gradient of 5–80% (v/v) acetonitrile containing 0.1% (v/v) formic acid at a flow rate of 0.2  $\mu$ l/min. The full mass scan range mode for tandem mass spectrometry was  $m/z = 450$ –2000Da. After determination of the charge states of an ion on zoom scans, product ion spectra were acquired in MS/MS mode with a relative collision energy of 55%. The individual spectra from MS/MS were processed using the

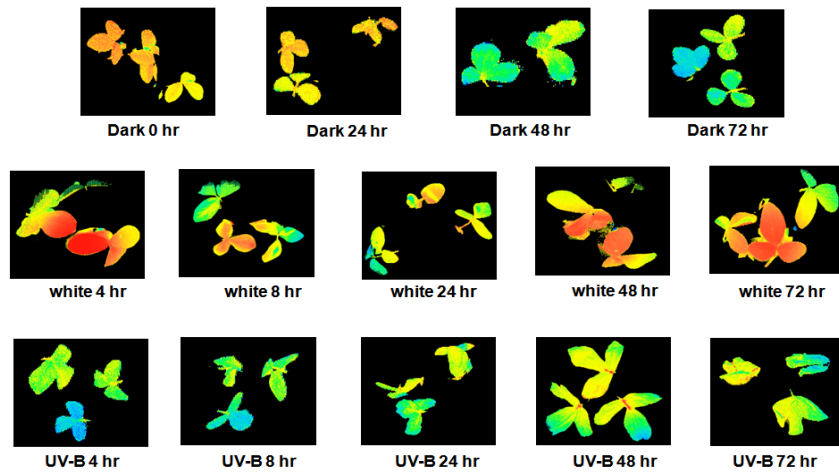


**Fig 7.** Fluorescent images of maximum quantum efficiency of PSII photochemistry ( $F_v/F_m$ ) during fluorescence quenching analysis. Higher energy fluorescence appeared red and lower as blue.

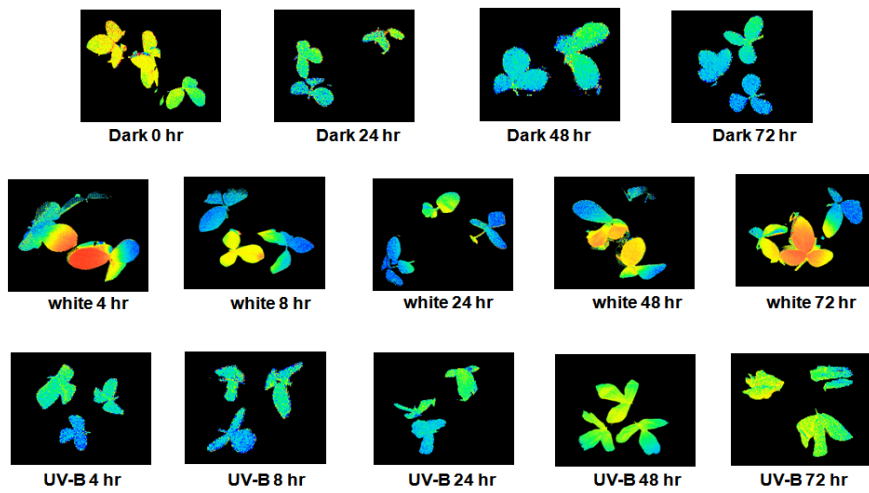


**Fig 8.** Fluorescence images of PSII operating efficiency ( $\Phi_{PSII}$ ) during fluorescence quenching analysis. Higher energy fluorescence appeared red and lower as blue.

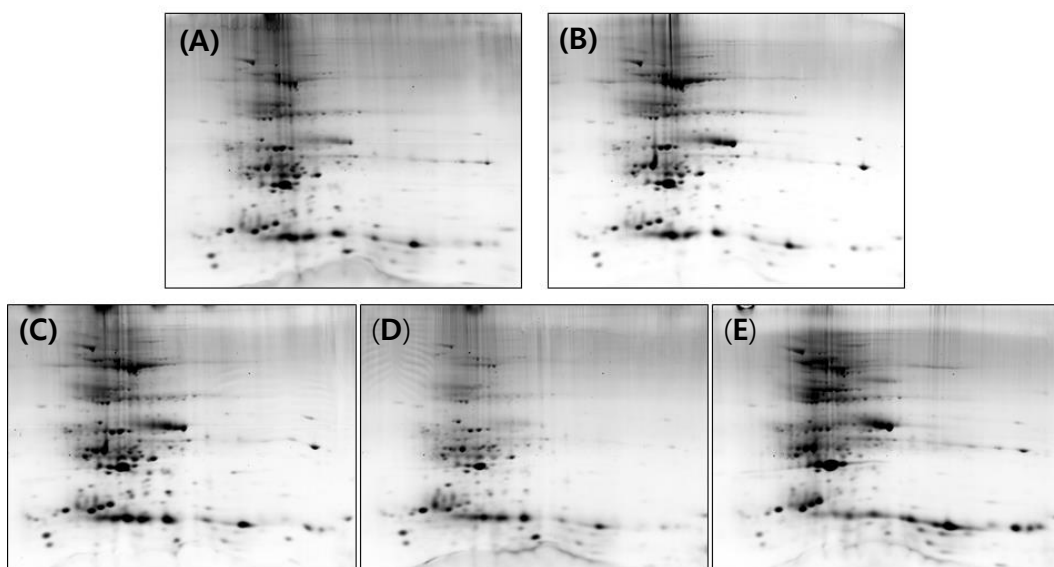


**Fig 9.** 2D-PAGE images of soybean leaves under the dark conditions. (A) 0 h after dark treatment; (B) 48 h after dark treatment; (C) 72 h after dark treatment. (D) Soybean leaves under continuous illumination of UV-B light for 72 h after 72 h of dark treatment. (E) Soybean leaves under continuous illumination of moderate light after 72 h of dark treatment.



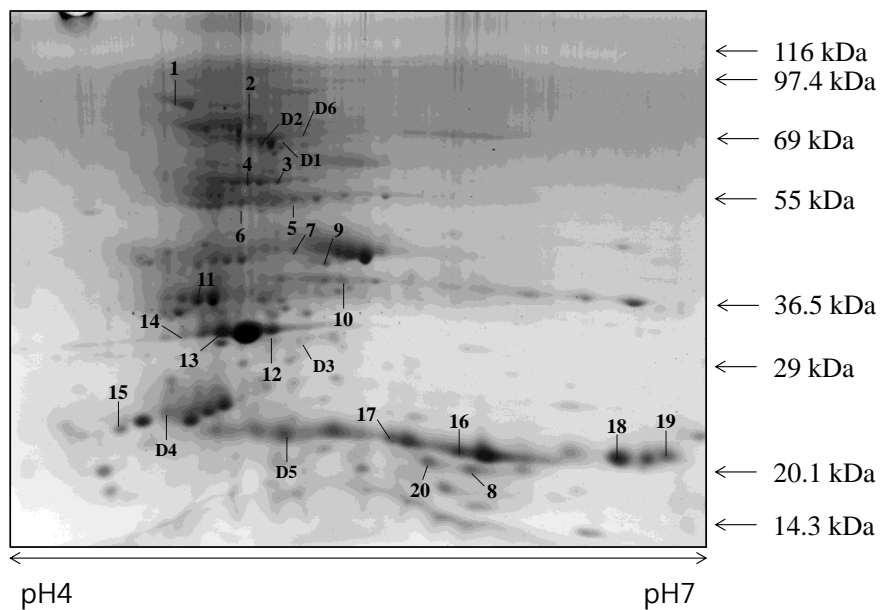


**Fig 10.** 2D-PAGE images of differentially expressed proteins in soybean leaves under UV-B radiation. Numbers without a D prefix indicate proteins that increased under UV-B radiation. Numbers with a D prefix indicate proteins that decreased under UV-B radiation.

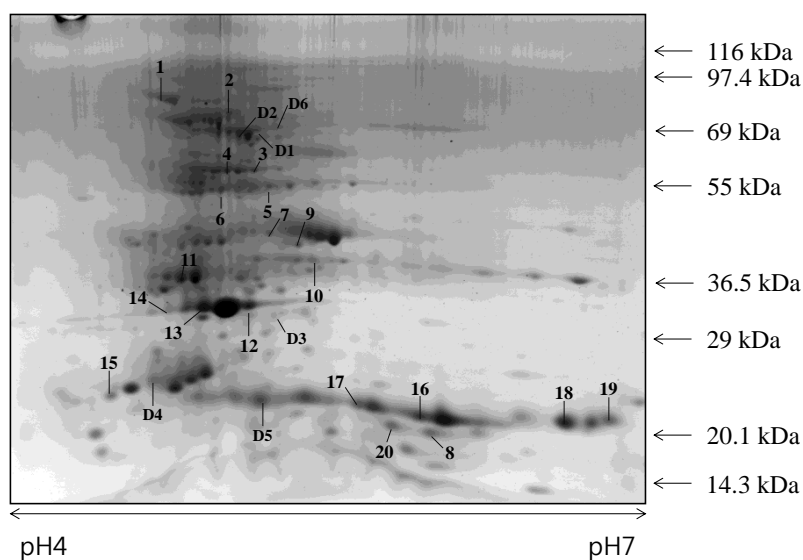


**Fig 11.** 2D-PAGE images of differentially expressed proteins in soybean leaves under moderate light. Numbers without a D prefix indicate proteins that increased under moderate light. Numbers with a D prefix indicate proteins that decreased under moderate light.

TurboSEQUEST software (Thermo Quest, San Jose, CA). The generated peak list files were used to query either the MSDB database or NCBI using the MASCOT program (<http://www.matrixscience.com>). Modifications of methionine and cysteine, a peptide mass tolerance at 2 Da, MS/MS ion mass tolerance at 0.8 Da, allowance of missed cleavage at 2, and charge states (+1, +2, and +3) were taken into account. Only significant hits as defined by MASCOT probability analysis were considered initially.

### Conclusions

Excessive UV-B radiation resulted in changes of the proteome in soybean leaves and caused over-production of carotenoids and anthocyanins to protect against photo-damage. UV-B radiation decreased chlorophyll a and b pigments and

chlorophyll a,b-binding protein in PS II, resulting in a decrease of light harvesting efficiency in soybean leaves. During climate change, UV-B may lead to hypo-production of agricultural commodities; thus, it should be carefully monitored.

### Acknowledgements

This paper is written based on Academic Funding Program supported by Academic Affair office of Hankyong National University.

### Competing Interests

The authors have declared that no competing interest exists.

## References

- Armond PA, Bjorkman O, Staehelin LA (1980) Dissociation of supramolecular complexes in chloroplast membranes. A manifestation of heat damage to the photosynthetic apparatus. *Biochim Biophys Acta* 601: 433–443.
- Bahk YY, Kim SA, Kim JS, Euh HJ, Bai GH, Cho SN, Kim YS (2004) Antigens secreted from *Mycobacterium tuberculosis*: Identification by proteomics approach and test for diagnostic marker. *Proteomics* 4: 3299–3307.
- Baker NR, Rosenqvist E (2004) Applications of chlorophyll fluorescence can improve crop production strategies: an examination of future possibilities. *J Exp Bot* 55: 1607–1621.
- Britton G (1993) Carotenoids in chloroplast pigment-protein complexes. In C. Sundqvist, ed, *Pigment-protein complexes in plastids: Synthesis and assembly*. Cell biology: A series of monographs. Academic press, San Diego, CA, pp 447–483.
- Calatayud A, Barreno E (2001) Chlorophyll a fluorescence, antioxidant enzymes and lipid peroxidation in tomato in response to ozone and benomyl. *Environ Pollut* 115:283–289.
- Casati P, Campi M, Morrow DJ, Fernandes J, Walbot V (2011) Transcriptomic, proteomic and metabolomics analysis of maize responses to UV-B. *Plant Signal Behav* 6:1146–1153.
- Close DC, Beadle CL (2003) The ecophysiology of foliar anthocyanin. *The Bot Rev* 69:149–161.
- Gao Y, Xiong W, Li XB, Gao CF, Zhang YL, Li H, Wu QY (2009) Identification of the proteomic changes in *Synechocystis* sp. PCC 6803 following prolonged UV-B irradiation. *J Exp Bot* 60:1141–1154.
- Gobom J, Nordhoff E, Mirgorodskaya E, Ekman R, Roepstroff P (1999) Sample purification and preparation technique based on nano-scale reversed-phase columns for the sensitive analysis of complex peptide mixtures by matrix-assisted laser desorption/ionization mass spectrometry. *J Mass Spectrom* 34:105–116.
- González JA, Gallardo MG, Boero C, Liberman Cruz M, Prado FE (2007) Altitudinal and seasonal variation of protective and photosynthetic pigments in leaves of the world's highest elevation trees *Polylepis tarapacana* (Rosaceae). *Acta Oecol* 32:36–41.
- Havaux M (1993) Characterisation of thermal damage to the photosynthetic electron transport system in potato leaves. *Plant Sci* 94:19–33.
- Henley WJ, Levavasseur G, Franklin LA, Osmond CB, Ramus J (1991) Photoacclimation and photoinhibition in *Ulva rotundata* as influenced by nitrogen availability. *Plant* 184: 235–343.
- Jansson S (1994) The light-harvesting chlorophylla/b-binding proteins. *Biochim Biophys Acta* 1194:1–19.
- Kim YJ, Lee JH, Lee OR, Shim JS, Jung SK, Son NR, Kim JH, Kim SY, Yang DC (2010) Isolation and characterization of a type II peroxiredoxin gene from *Panax ginseng* C. A. Meyer. *J Ginseng Res* 34:296–303.
- Kerr JB, McElroy CT (1993) Evidence for large upward trends of ultraviolet-B radiation linked to ozone depletion. *Science* 262:1032–1034.
- Kim J, Cho HK, Lee YG, Oh SN, Baek SK (2005) Updated trends of stratospheric ozone over Seoul. *J. Atmosphere* 15:101–118.
- Kim CG, Lee SM, Jeong HK, Jang JK, Kim YH, Lee CK (2010) Impacts of climate change on Korean agriculture and counterstrategies. Research Report R593, Korea Rural Economic Institute, Munwonsa, Seoul, Korea, 282 pp.
- Kim SJ, Park TY, Kim SM, Kim SM (2012) The proxy variable selection of vulnerability assessment for agricultural infrastructure according to climate change. *KCID J* 18:33–42.
- Krause GH, Schmude C, Garden H, Koroleva OY, Winter K (1999) Effects of solar ultraviolet radiation on the potential efficiency of photosystems II in leaves of tropical plants. *Plant Physiol* 121:1349–1358.
- Kubo E, Hasanova N, Tanaka Y, Fatma N, Takamura Y, Singh DP, Akagi Y (2010) Protein expression profiling of lens epithelial cells from Prdx6-depleted mice and their vulnerability to UV radiation exposure. *Am J Physiol Cell Physiol* 298:C342–354.
- Lichrtenthaler HK, Ac A, Marek MV, Kalina J, Urban O (2007) Differences in pigment composition, photosynthetic rates and chlorophyll fluorescence images of sun and shade leaves of four tree species. *Plant Physiol Biochem* 45:577–588.
- Mewis I, Schreinder M, Nguyen CN, Krumbein A, Ulrichs C, Loshe M, Zrenner R (2012) UV-B irradiation changes specifically the secondary metabolite profile in broccoli sprouts: induced signaling overlaps with defense response to biotic stressors. *Plant Cell Physiol* 53:1546–1560.
- Middleton EM, Teramura AH (1993) The role of flavonol glycosides and carotenoids in protecting soybean from ultraviolet-B damage. *Plant Physiol*. 103:741–752.
- Mishra Y, Chaurasia N, Rai LC (2009) Heat pretreatment alleviates UV-B toxicity in the cyanobacterium *Anabaena doliolum*: A proteomic analysis of cross tolerance. *Photochem Photobiol* 85:824–833.
- Panda D, Sharma SG, Sarkar RK (2008) Chlorophyll fluorescence parameters, CO<sub>2</sub> photosynthetic rate and regeneration capacity as a result of complete submergence and subsequent re-emergence in rice (*Oryza sativa* L.). *Aquat Bot* 88:127–133.
- Park YD, Kim SY, Jung HS, Seo EY, Namkung JH, Park HS, Cho SY, Park YK, Yang JM (2004) Towards a proteomic analysis of atopic dermatitis: A two-dimensional-polyacrylamide gel electrophoresis/mass spectrometric analysis of cultured patient-derived fibroblasts. *Proteomics* 4:3446–3455.
- Rintamaki E, Salo R, Lehtonen E, Aro EM (1995) Regulation of D1 protein-degradation during photoinhibition of photosystem-I in-vivo-phosphorylation of D1 protein in various plant groups. *Planta* 195:379–386.
- Schenk G, Duggleby RG, Nixon PF (1998) Properties and functions of the thiamin diphosphate dependent enzyme transketolase. *Int J Biochem Cell Biol* 30:1297–1318.
- Schreiber U, Schliwa U, Bilger W (1986) Continuous recording of photochemical and nonphotochemical chlorophyll fluorescence quenching with a new type of modulation fluorometer. *Photosynth Res* 10:51–62.
- Sims DA, Gamon JA (1999) Estimating chlorophyll, carotenoid and anthocyanin concentration using hyperspectral reflectance. Annual Meeting of the Ecological Society of America, pp. 8–12.
- Singh A, Sarkar A, Singh S (2010) Investigation of supplemental ultraviolet-B-induced changes in antioxidative defense system and leaf proteome in radish (*Raphanus sativus* L. cv Truthful): an insight to plant response under high oxidative stress. *Protoplasma* 245:75–83.
- Xu C, Sullivan JH, Garnett WM, Caperna TJ, Natarajan S (2008) Impact of solar ultraviolet-B on the proteome in soybean lines differing in flavonoid contents. *Phytochemistry* 69:38–48.
- Zuo X, Echan L, Hembach P, Tang HY, Speicher KD, Santoli D, Speicher DW (2001) Towards global analysis of mammalian proteomes using sample prefractionation prior to narrow pH range two-dimensional gels and using one-dimensional gels for insoluble and large proteins. *Electrophoresis* 22:1603–1615.